PERGAMON

Planetary and Space Science 49 (2001) 743–748

Planetary and Space Science

www.elsevier.nl/locate/planspasci

The topography and gravity of Mare Serenitatis: implications for subsidence of the mare surface

Thomas R. Watters[a, *], Alex S. Konopliv[b]

[a] *Center for Earth and Planetary Studies, National Air and Space Museum, Smithsonian Institution, Washington, DC 20560-0315, USA*
[b] *Jet Propulsion Laboratory, California Institute of Technology, Pasadena, CA 91109, USA*

Received 6 October 2000; accepted 19 December 2000

Abstract

The long wavelength topography of Mare Serenitatis was analyzed using topographic data obtained by the Clementine laser ranging instrument (LIDAR). The topography shows that the lowest elevations in the mare surface occur near the margins of the basin. The present mare surface reflects a long period of volcanism, subsidence, and deformation. Subsidence is generally attributed to a Gaussian-shaped, superisostatic load from the mare basalts that results in flexure of the lunar lithosphere. Gravity data from Lunar Prospector suggest that the basalt sequence in the interior of Serenitatis is generally uniform in thickness and thins rapidly at the margins. This suggests that the topographic lows in the basin do not coincide with areas where the mare basalts are thick but rather occur where the basalts thin. The topographic lows also do not appear to coincide with accumulations of the youngest mare basalt units. The long wavelength topography of Mare Serenitatis may reflect subsidence influenced by pre-mare basalt basin topography and preexisting zones of lithospheric weakness.

1. Introduction

Mare Serenitatis is one of the largest and most circular maria on the Moon (Fig. 1). It is approximately 600 km in diameter and has a ring structure that may extend out to 880 km (see Solomon and Head, 1979, Fig. 2). Based on its degraded appearance, the Serenitatis basin is thought by some to be one of the oldest on the Moon (Wilhelms, 1987). However, radiometric ages of Apollo 17 samples suggest that it is a young basin (Staudacher et al., 1978). The mare basalts that subsequently flooded the Serenitatis basin are dominated by two tectonic landforms, mare ridges (or wrinkle ridges) and arcuate rilles. Mare ridges are found in nearly all lunar maria and typically occur both radial to and concentric with the centers of circular mare filled basins (Strom, 1972; Bryan, 1973; Maxwell et al., 1975). They are generally thought to be compressional features (Bryan, 1973; Howard and Muehlberger, 1973; Muehlberger, 1974; Maxwell et al., 1975; Lucchitta, 1976, 1977; Maxwell and Phillips, 1978; Sharpton and Head, 1982, 1988) resulting from a combination of folding and thrust faulting (Plescia and Golombek, 1986; Watters, 1988; Golombek et al., 1991; Watters, 1991; Watters and Robinson, 1997; Schultz, 2000). Arcuate rilles are linear to arcuate troughs with flat floors and steep walls (see Wilhelms, 1987). These troughs are interpreted to be graben formed by extensional stresses (Baldwin, 1963; McGill, 1971; Golombek, 1979). Lunar graben have a simple geometry and often occur in parallel or echelon sets, concentric to circular maria (Golombek, 1979; Wilhelms, 1987). Most lunar graben are located along basin rims and cut both mare and basin material (Wilhelms, 1987).

The origin of the stresses that formed the mare ridges and arcuate graben associated with mascon maria is generally thought to be due to subsidence of the mare basalts (Bryan, 1973; Maxwell et al., 1975; Lucchitta, 1976, 1977; Maxwell, 1978), although global contraction or a combination of subsidence and global contraction have also been suggested (Muehlberger, 1974; Solomon and Head, 1978). In an effort to evaluate the pattern and nature of subsidence of the mare surface, the long wavelength topography of Mare

* Corresponding author. Tel.: +1-202-357-1425; fax: +1-202-786-2566.
E-mail address: twatters@nasm.si.edu (T. R. Watters).

0032-0633/01/$ - see front matter
PII: S0032-0633(01)00007-1

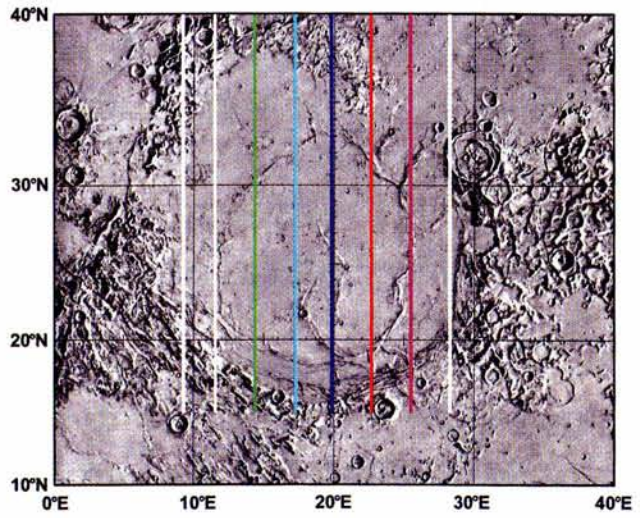

Fig. 1. Shaded relief map of Mare Serenitatis. Mare Serenitatis is about 600 km in diameter and a prominent system of wrinkle ridges dominate the mare surface. The vertical lines are the locations of LIDAR profiles, those lines coded by color indicate the locations of profiles shown in Fig. 2.

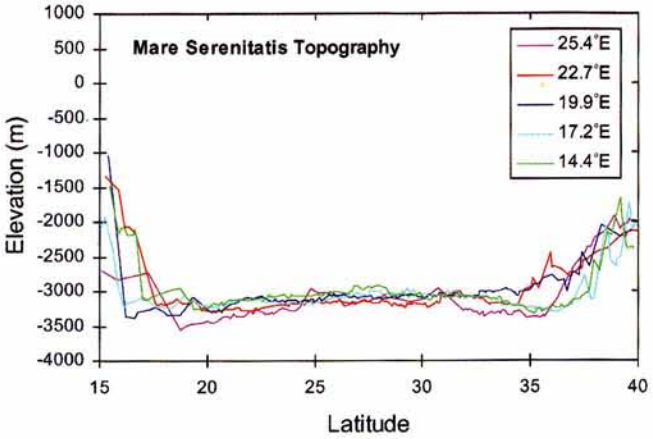

Fig. 2. LIDAR profiles crossing Mare Serenitatis. Profiles are portions of the LIDAR data in orbital tracks located at about 14.4°E, 17.2°E, 19.9°E, 22.7°E, and 25.4°E longitude. Profile locations are shown in Fig. 1. The LIDAR data were extracted from the data set of Smith et al. (1997). Elevations are in meters above an ellipsoid of radius 1738 km at the equator with a flattening of 1/3234.93 corresponding to the flattening of the geoid, and the vertical exaggeration is 80:1.

Serenitatis is analyzed using topographic data obtained by the laser ranging instrument (LIDAR) flown on the Clementine spacecraft. The characteristics of the mare fill and the subsurface structure of Mare Serenitatis is also inferred from Lunar Prospector gravity data.

2. Observations

2.1. Topography

The LIDAR instrument has provided a wealth of new topographic data for the Moon between 75°S and 75°N latitude (see Nozette et al., 1994). Clementine's polar orbit provided altimetry data along north–south orbital tracks (roughly along lines of longitude) spaced by approximately 2.5° at the equator (Zuber et al., 1994; also see Spudis et al., 1994). Overlapping coverage exists for some areas providing profiles that are spaced by only a few tenths of a degree. The laser had a surface spot size of ~200 m at the minimum spacecraft altitude, and an along track shot spacing, assuming a 100% laser ranging probability, of ~20 km over smooth mare surfaces and ~100 km over rough highland terrains (Smith et al., 1997). Because of the influence of terrain roughness and solar phase angle, the distribution of good returns is highly variable within an orbital track. Spudis et al. (1994) estimate that within an orbital track, valid topographic measurements may make up as little as 15% of the total returns in very rough terrain near zero solar phase angle or nearly 100% of the returns for smooth maria overflown late in the mission when solar phase angles were larger. Although the distributions of valid returns and thus the spatial resolution within an orbital track is variable, the single-shot ranging precision of the LIDAR is 40 m and the absolute vertical accuracy is estimated to be 100 m (Zuber et al., 1994; Smith et al., 1997). The LIDAR data are the best elevation data available for Mare Serenitatis since the accuracy of stereo-derived data are limited over relatively featureless mare surfaces (Cook and Robinson, 1999).

LIDAR data (from Smith et al., 1997) along eight orbital tracks that cross Mare Serenitatis have been examined (Fig. 1). The long wavelength topography shown in LIDAR profiles that cross the interior of Serenitatis indicate that the center of the mare is higher than the margins (Fig. 2). In the 25.4°E longitude profile, the elevation difference between the center of the mare and the lowest elevation of the mare surface is up to 400 m (Fig. 2). An exception to this trend is reflected in the 19.9°E longitude profile (Fig. 2) that shows a general increase in elevation of the mare surface from south to north. A digital elevation model (DEM) of Mare Serenitatis was extracted from the global lunar DEM generated using the LIDAR data by Smith et al. (1997). The global lunar DEM has grid resolution of 0.25° × 0.25°, corresponding to the minimum spacing between orbital passes (Smith et al., 1997). The DEM of Mare Serenitatis indicates that much of the northern, eastern, and southern margins are lower than the center of the mare (Fig. 3). East–west trends in the topography across the central basin, however, indicate a less prominent central topographic high and, in some areas, a gradual decrease in elevation of the mare surface from west to east (Fig. 3). This trend was first revealed in Apollo Laser Altimeter data (see Wollenhaupt et al., 1973, Fig. 33-24a) and Apollo Lunar Sounder Experiment (ALSE) data (see Sharpton, 1992, Fig. 2). The lowest point in Mare Serenitatis is located on its southeast margin, over 400 m below the center of the mare (Fig. 3). If the long wavelength topography of the mare surface is due to subsidence of the basalts, the topographic data suggest that significant

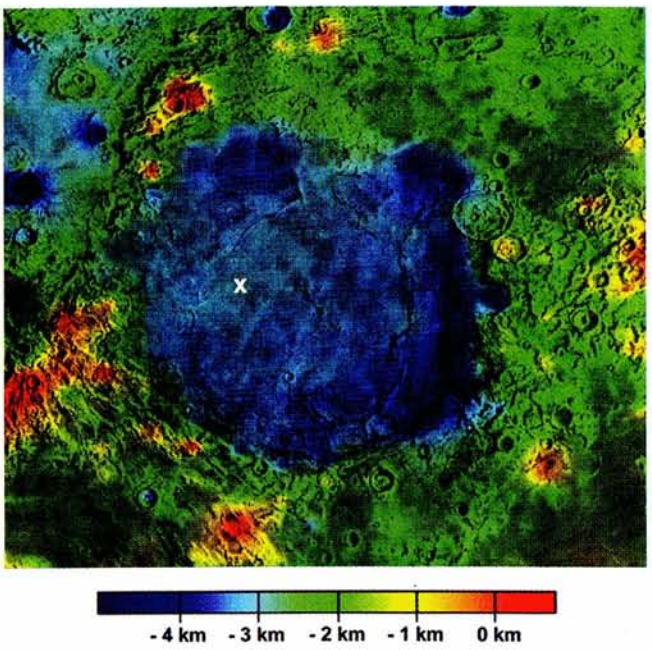

Fig. 3. Digital elevation model (DEM) of Mare Serenitatis. The DEM was extracted from the global lunar DEM generated by Smith et al. (1997) and is overlaid on the shaded relief map. The lowest elevations on the mare surface are located near the margins. The white "X" shows the approximate location of the highest elevation in the interior of the mare. Elevations are in meters above an ellipsoid of radius 1738 km at the equator, with a flattening of 1/3234.93 corresponding to the flattening of the geoid.

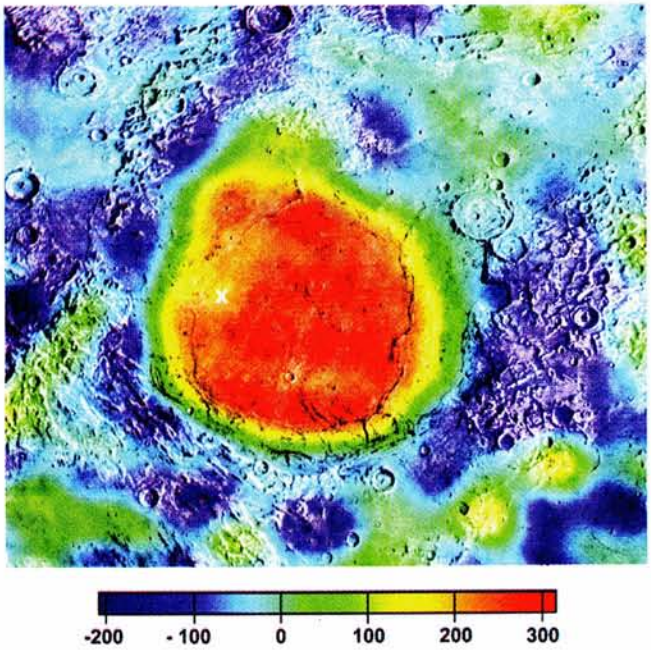

Fig. 4. Free-air gravity derived from the Lunar Prospector 165th degree gravity model (LP165P) (Konopliv et al., 2001). The grid was generated by truncating LP165P at degree and order 110. Gravity is overlaid on the shaded relief map. The plateau-shaped positive anomaly is located in the interior of the basin and roughly coincides with the mare basalts inside the prominent ridge ring. The white "X" shows the approximate location of a relative low or ledge in the anomaly (see Fig. 5). Units are in milligals.

subsidence has occurred along the margins, particularly along the southeast margin.

In general, the lowest elevations in the mare lie outside the prominent mare ridge ring in the interior of Serenitatis. The elevation of the mare surface on the margin-side of the pronounced eastern segments of the ridge ring, made up of Dorsa Lister and Smirnov, is invariably lower than the interior-side (Fig. 3). This trend does not hold for mare ridges along the margins of Serenitatis. Dorsa Aldrovandi, for example, is located on the western margin of Serenitatis and here the elevation of the mare surface on the margin-side of the ridge is higher than the interior-side (see Fig. 3).

2.2. Gravity

Gravitational field models derived from data collected by the Lunar Orbiters, the Apollo missions, Clementine, and most recently from the Lunar Prospector mission, indicate that the Serenitatis mascon, like others, has a strong positive gravity anomaly ringed by a negative anomaly (Zuber et al., 1994, Fig. 2b; Lemoine et al., 1997, Plate 1; Konopliv et al., 1998, Fig. 1a). The positive anomaly is attributed to the uncompensated mare basalts (Phillips et al., 1972) and the presence of a dense mantle "plug" formed by post-impact mantle rebound (Wise and Yates, 1970; Solomon and Head, 1979) (for a summary discussion of the relative contribution of mantle material and the basalt fill to the gravity see Konopliv et al., 1998). The uncompensated basalts, supported by the flexural strength of the lunar lithosphere, result in the downward deflection of the lithosphere and compressional stresses in the interior of the basin that form the wrinkle ridges and extensional stresses on the margins that form arcuate graben (Melosh, 1978; Solomon and Head, 1979, 1980). A positive free-air gravity anomaly supports a mascon tectonic model involving flexure of the lithosphere due to loading of the mare basalts, and the surrounding negative anomaly suggests subsurface mass deficiencies that result from crustal thickening related to basin formation or modification (Lemoine et al., 1997).

Evidence such as a decrease in the number of pre-mare craters, gravity, and ALSE subsurface profiles have led to the conclusion that the basalts have the greatest thickness in the centers of the basins (see Baldwin, 1970; Wilhelms, 1987). The gravity model of Lemoine et al. (1997) (GLGM-2 free-air model) is consistent with previous models that indicate a "bull's eye" pattern with the high located roughly in the center of Serenitatis. If the dominant contribution to the gravity anomaly is from the basalt fill (Phillips et al., 1972), this pattern would suggest an axially symmetric, Gaussian-shaped accumulation with the greatest thickness of the basalts near the basin center. The most recent gravity models (Konopliv et al., 1998, 2001; Konopliv and Yuan, 1999), however, show that the anomaly for Serenitatis does not have a "bull's eye" pattern (Fig. 4).

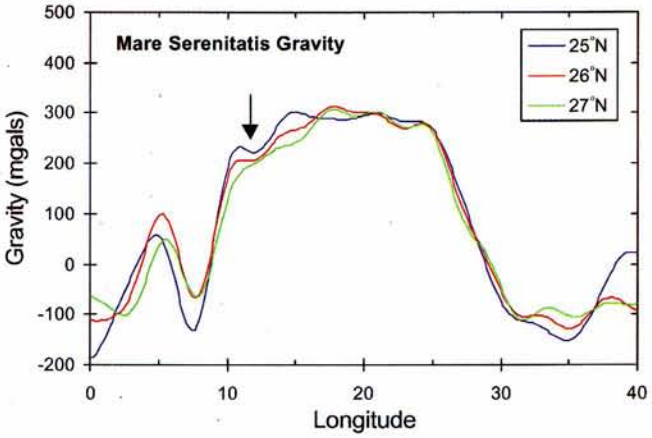

Fig. 5. Plots of the free-air gravity over Mare Serenitatis. The plots are along 25°N, 26°N, and 27°N latitude (see legend). The anomaly has a plateau shape in the interior of the basin and steep shoulders near the basin margins (see Fig. 4). The arrow shows the location of a ~60 mgal relative low in the positive anomaly that roughly coincides with the location of the highest elevation of the interior mare surface (see Fig. 3). Units are in milligals.

The anomaly is a broad plateau over the mare interior, roughly corresponding to the area inside the mare ridge ring (Fig. 5). The shape of the anomaly, particularly the strong shoulders near the margins, supports interpretations that it is dominated by the near-surface mare fill (Phillips et al., 1972; Konopliv et al., 1998). If this is the case, the basalt sequence in the interior of the basin may be generally uniform in thickness and thin rapidly at the margins; a shape not well approximated by an axially symmetric Gaussian-shaped sequence. Thus, the topographic lows in the mare surface do not appear to coincide with areas where the basalts are thick. They occur where the gravity data suggest the basalt sequence is thinning. The gravity data also suggest that the pre-mare basalt topography of the interior of Serenitatis may have been more flat than bowl shaped. Although this interpretation of the subsurface structure is non-unique, it is consistent with the available data. Gravity data for Crisium, Humorum, Imbrium, and Nectaris suggest that the mare fill in these basins may also be roughly uniform in thickness and better approximated by broad tabular-shaped basalt sequences (Konopliv et al., 1998, 2001).

3. Discussion

The observation that mare surfaces fall close to an ellipsoidal surface lead to the hypothesis that mare basalts originated in the deep interior and flooded Serenitatis and the other nearside basins to an equipotential level (Runcorn, 1974; Sjogren and Wollenhaupt, 1976; Brown et al., 1974; Smith et al., 1997). A recent analysis by Arkani-Hamed et al. (1999) suggests that basins flooded to local rather than a global equipotential surface. Although the mare basalts filled the Serenitatis basins to an equipotential level, the total accumulation of the mare sequence is estimated to have occurred over a period of 800 myr (Howard et al., 1973; Solomon and Head, 1979, 1980) to 1.4 byr (Hiesinger et al., 2001). As the basalts flooded the basin over this period, the newly formed mare floors subsided. Subsidence was thus contemporaneous with the emplacement of the mare sequence. Solomon and Head (1979, 1980) suggested the following sequence of events in the evolution of Mare Serenitatis. The oldest basalt units were emplaced from about 3.85 to 3.65 byr ago. Subsidence of these basalts resulted in the basin concentric graben. Intermediate age basalt units were emplaced about at 3.5 byr, filling the centrally subsiding depression, extending out to the basin margins, and embaying many of the graben formed in the oldest basalt units. The youngest basalts flooded the interior of the basin at about 3.4–3.0 byr. Subsidence continued during and after the emplacement of the intermediate and youngest units, forming the mare ridges. Units in Mare Serenitatis estimated to be younger than 3.0 byr have been identified (Boyce, 1976) and some may be as young as 2.44 byr (Hiesinger et al., 2001). The total thickness of the basalt sequence in Serenitatis and other mascon maria is estimated to be 2–4 km or as much as 3–6 km (Sjogren et al., 1974; Solomon and Head, 1979, 1980; Arkani-Hamed, 1998; Williams and Zuber, 1998). Thus, the present surface of Mare Serenitatis reflects a long period of volcanism, subsidence, and deformation.

The long wavelength topography of the mare surface may be dominated by the last stages of flooding and subsidence. If this is the case, the topographic lows in Mare Serenitatis may be the result of subsidence in response to the emplacement of young basalt units near the margins. The basalt units exposed at the margins are, however, for the most part intermediate to old in age (Boyce, 1976, Fig. 4; Solomon and Head, 1979, Fig. 4; Hiesinger et al., 2001, Fig. 9). Exceptions may be some small areas on the eastern margin, south of Posidonius, where young mare basalt units are exposed (Boyce, 1976, Fig. 4; Hiesinger et al., 2001, Fig. 9). This suggests that the topographic lows in the mare surface and the distribution of young mare units is not strongly correlated.

The observed topographic high in the west-central portion of Serenitatis may represent a late-stage, localized accumulation of mare basalts. Solomon and Head (1979, Fig. 4) mapped the basalt units exposed in the area of the topographic high as mostly intermediate in age. Boyce (1976, Fig. 4) concluded that the basalts in this area are younger than the central mare unit. Hiesinger et al. (2001) mapped units in west-central Serenitatis that are intermediate to young in age, ranging from 3.6 to 2.9 byr. Gravity data indicate a ~60 mgal relative low in the positive anomaly (Figs. 4 and 5) that roughly corresponds to the topographic high (Fig. 3). This relative low or ledge in the anomaly suggests that the sequence of basalts may be thinner in this area, possibly overlying a topographic high in the basin floor composed of less dense crustal material. The topographic high may be due to a relatively thin accumulation of intermediate to young mare basalts that did not subside appreciably after emplacement.

Subsidence may have been influenced by pre-mare basalt basin topography and pre-existing zones of weakness in the lunar lithosphere. The most significant influence on the pre-mare basalt topography and zones of lithospheric weakness may have been from the formation of pre- and post-Serenitatis basins. Based on photogeologic evidence and gravity data, Scott (1974) suggested that Serenitatis is a composite of two independent basins; a North and South Serenitatis (also see Spudis, 1993). The northern basin is older and smaller than the southern basin, and its northern rim corresponds to the northwestern rim of Serenitatis (see Scott, 1974, Fig. 1). The proposed location of the northern basin correlates well with the topographic low on the northwestern margin of Serenitatis. It also roughly corresponds to a ~ 160 mgal feature in the Serenitatis gravity anomaly (Fig. 4). The gravity data suggest that the mare fill is significantly thinner in this area relative to the interior of Serenitatis. Thus, the gravity and topography support the idea that Serenitatis is made up of two overlapping basins.

The ring system of the Imbrium basin may have also contributed to the topography of Mare Serenitatis. Spudis (1993) suggests that the prominent topography of the eastern rim of Serenitatis may be due to the coincident alignment of its ring system with the large, outer rings of Imbrium. The intersection between Serenitatis and Imbrium basin rings are thought to have produced an uplifted section of the pre-Imbrian crust within the Apennines (southwest margin of Serenitatis) (see Spudis, 1993), and the Imbrium ring system may have contributed to the elevated topography in western Serenitatis.

If the topographic lows along the eastern margin of Serenitatis are not due to subsidence of young mare basalts, they may reflect subsidence influenced by a zone of weakness in the pre-mare basin floor. Such a zone of weakness could have been formed by the alignment of an outer ring of Imbrium with the eastern margin of Serenitatis. This might help account for the topographic lows in the mare surface where the basalt sequence is relatively thin.

Acknowledgements

We thank B. Ray Hawke and an anonymous reviewer for their reviews of the manuscript, and Anthony C. Cook for his help with generating some of the figures. This research was supported by Grants from National Aeronautics and Space Administration. Research by ASK was carried out by the Jet Propulsion Laboratory, California Institute of Technology, under a contract with the National Aeronautics and Space Administration.

References

Arkani-Hamed, J., 1998. The lunar masons revisited. J. Geophys. Res. 103, 3709–3739.

Arkani-Hamed, J., Konopliv, A.S., Sjogren, W.L., 1999. On the equipotential surface hypothesis of lunar maria floors. J. Geophys. Res. 104, 5921–5931.

Baldwin, R.B., 1963. The measure of the Moon. University of Chicago Press, Chicago.

Baldwin, R.B., 1970. A new method of determining the depth of the lava in lunar maria. Astron. Soc. Pacific Publication 82, 857–864.

Boyce, J.M., 1976. Ages of flow units in the lunar nearside maria based on Lunar Orbiter IV photographs. Proceedings of the Seventh Lunar Science Conference. pp. 2717–2728.

Brown, W.E. Jr., Adams, G.F., Eggleton, R.E., Jackson, P., Jordan, R., Kobrick, M., Peeples, W.J., Phillips, R.J., Porcello, L.J., Schaber, G., Sill, W.R., Thompson, T.W., Ward, S.H., Zelenka, J.S., 1974. Elevation profiles of the Moon. Proceedings of the Fifth Lunar Science Conference. pp. 3037–3048.

Bryan, W.B., 1973. Wrinkle-ridges as deformed surface crust on ponded mare lava. Proceedings of the Fourth Lunar Science Conference. pp. 93–106.

Cook, A.C., Robinson, M.S., 1999. Elevation models of the lunar surface (abstract). New views of the Moon II. Lunar Planetary Institute [CD-ROM], p. 8056.

Golombek, M.P., 1979. Structural analysis of lunar grabens and the shallow crustal structure of the Moon. J. Geophys. Res. 84, 4657–4666.

Golombek, M.P., Plescia, J.B., Franklin, B.J., 1991. Faulting and folding in the formation of planetary wrinkle ridges. Proceedings of the 21st Lunar and Planetary Science Conference. pp. 679–693.

Hiesinger, H., Jaumann, R., Neukum, G., Head, J.W., 2001. Ages of mare basalts on the lunar nearside. J. Geophys. Res. 105, 29,239–29,275.

Howard, K.A., Muehlberger, W.R., 1973. Lunar thrust faults in the Taurus–Littrow region. Apollo 17 Preliminary Science Report, NASA SP-330, pp. 31-32–31-25.

Howard, K.A., Carr, M.H., Muehlberger, W.R., 1973. Basalt stratigraphy of southern Mare Serenitatis. Apollo 17 Preliminary Science Report, NASA SP-330, pp. 29-1–29-12.

Konopliv, A.S., Asmar, S.W., Carranza, E., Sjogren, W.L., Yuan, D.N., 2001. Recent gravity models as a result of the Lunar Prospector Mission. Icarus in press.

Konopliv, A.S., Binder, A.B., Hood, L.L., Kucinskas, A.B., Sjogren, W.L., Williams, J.G., 1998. Improved gravity field of the Moon from Lunar Prospector. Science 281, 1476–1480.

Konopliv, A.S., Yuan, D.N., 1999. Lunar Prospector 100th Degree Gravity Model Development. Proceedings of the 30th Lunar and Planetary Science Conference. pp. 1067–1068.

Lemoine, F.G.R., Smith, D.E., Zuber, M.T., Neumann, G.A., Rowlands, D.D., 1997. A 70th degree lunar gravity model (GLGM-2) from Clementine and other tracking data. J. Geophys. Res. 102, 16,339–16,359.

Lucchitta, B.K., 1976. Mare ridges and related highland scarps-results of vertical tectonism. Proceedings of the Seventh Lunar Science Conference. pp. 2761–2782.

Lucchitta, B.K., 1977. Topography, structure, and mare ridges in southern Mare Imbrium and northern Oceanus Procellarum. Proceedings of the Eighth Lunar Science Conference. pp. 2691–2703.

Maxwell, T.A., 1978. Origin of multi-ring basin ridge systems: an upper limit to elastic deformation based on a finite-element model. Proceedings of the Ninth Lunar and Planetary Science Conference. pp. 3541–3559.

Maxwell, T.A., El-Baz, F., Ward, S.W., 1975. Distribution, morphology, and origin of ridges and arches in Mare Serenitatis. Geol. Soc. Am. Bull. 86, 1273–1278.

Maxwell, T.A., Phillips, R.J., 1978. Stratigraphic correlation of the radardetected subsurface interface in Mare Crisium. Geophys. Res. Lett. 5, 811–814.

McGill, G.E., 1971. Attitude of fractures bounding straight and arcuate lunar rilles. Icarus 14, 53–58.

Melosh, H.J., 1978. The tectonics of mascon loading. Proceedings of the Ninth Lunar and Planetary Science Conference. pp. 3513–3525.

Muehlberger, W.R., 1974. Structural history of southeastern Mare Serenitatis and adjacent highlands. Proceedings of the Fifth Lunar Science Conference. pp. 101–110.

Nozette, S., et al., 1994. The Clementine Mission to the Moon: scientific overview. Science 266, 1835–1839.

Phillips, R.J., Conel, J.E., Abbott, E.A., Sjogren, W.L., Morton, J.B., 1972. Masons: progress toward a unique solution for mass distribution. J. Geophys. Res. 77, 7106–7114.

Plescia, J.B., Golombek, M.P., 1986. Origin of planetary wrinkle ridges based on the study of terrestrial analogs. Geol. Soc. Am. Bull. 97, 1289–1299.

Runcorn, S.K., 1974. On the origin of mascons and moonquakes. Proceedings of the Fifth Lunar Science Conference. pp. 3115–3126.

Schultz, R.A., 2000. Localizaton of bedding plane slip and backthrusting faults above blind thrust faults: keys to wrinkle ridge structure. J. Geophys. Res. 105, 12,035–12,052.

Scott, D.H., 1974. The geologic significance of some lunar gravity anomalies. Proceedings of the Fifth Lunar Science Conference. pp. 3025–3036.

Sharpton, V.L., 1992. Apollo 17: one giant step toward understanding the tectonic evolution of the Moon. Geology of the Apollo 17 Landing Site, LPI Tech. Rep. 92-09, Part 1, pp. 50–53.

Sharpton, V.L., Head, J.W., 1982. Stratigraphy and structural evolution of southern Mare Serenitatis: a reinterpretation based on Apollo Lunar Sounder Experiment data. J. Geophys. Res. 87, 10,983–10,998.

Sharpton, V.L., Head, J.W., 1988. Lunar mare ridges: analysis of ridge-crater intersections and implications for the tectonic origin of mare ridges. Proceedings of the 28th Lunar and Planetary Science Conference. pp. 307–317.

Sjogren, W.L., Wimberly, R.N., Wollenhaupt, W.R., 1974. Lunar gravity via the Apollo 15 and 16 subsatellites. Moon 9, 115–128.

Sjogren, W.L., Wollenhaupt, W.R., 1976. Lunar global figure from mare surface elevations. Moon 15, 143–154.

Smith, D.E., Zuber, M.T., Neumann, G.A., Lemoine, F.G., 1997. Topography of the Moon from the Clementine LIDAR. J. Geophys. Res. 102, 1591–1611.

Solomon, S.C., Head, J.W., 1978. The nature of isostasy on the Moon: how big a Pratt-fall for airy models? Proceedings of the Ninth Lunar Science Conference. pp. 3499–3511.

Solomon, S.C., Head, J.W., 1979. Vertical movement in mare basins: relation to mare emplacement, basin tectonics, and lunar thermal history. J. Geophys. Res. 84, 1667–1682.

Solomon, S.C., Head, J.W., 1980. Lunar mascon basins: lava filling, tectonics, and evolution of the lithosphere. Rev. Geophys. Space Phys. 18, 107–141.

Spudis, P.D., 1993. The geology of multi-ring impact basins. Cambridge University Press, Cambridge.

Spudis, P.D., Reisse, R.A., Gillis, J.J., 1994. Ancient multiring basins on the Moon revealed by Clementine laser altimetry. Science 266, 1848–1851.

Staudacher, T., Dominik, B., Jessberger, E.K., Kirsten, T., 1978. Consortium breccia 73255: ^{40}Ar-^{39}Ar dating. Proceedings of the Ninth Lunar Science Conference. pp. 1098–1100.

Strom, R.G., 1972. Lunar mare ridges, rings and volcanic ring complexes. Modern Geology 2, 133–157.

Watters, T.R., 1988. Wrinkle ridge assemblages on the terrestrial planets. J. Geophys. Res. 93, 10,236–10,254.

Watters, T.R., 1991. The origin of periodically spaced wrinkle ridges on the Tharsis plateau of Mars. J. Geophys. Res. 96, 15,599–15,616.

Watters, T.R., Robinson, M.S., 1997. Radar and photoclinometric studies of wrinkle ridges on Mars. J. Geophys. Res. 102, 10,889–10,903.

Wilhelms, D.E., 1987. The geologic history of the Moon. US Govt. Print Office, Washington, DC.

Williams, K.K., Zuber, M.T., 1998. Measurement and analysis of lunar basin depths from Clementine altimetry. Icarus 131, 107–122.

Wise, D.U., Yates, M.T., 1970. Macons as structural relief on a lunar "Moho". J. Geophys. Res. 75, 261–268.

Wollenhaupt, W.R., Sjogren, W.L., Lingenfelter, R.E., Schubert, G., Kaula, W.M., 1973. Apollo 17 Laser Altimeter. Apollo 17 Preliminary Science Report, NASA SP-330, pp. 33-41–33-44.

Zuber, M.T., Smith, D.E., Lemoine, F.G., Neumann, G.A., 1994. The shape and internal structure of the Moon from the Clementine Mission. Science 266, 1839–1843.